Beached microplastics in the Northwestern Mediterranean Sea

Mel Constant, Philippe Kerhervé, Morgan Mino-Vercellio-Verollet, Marc Dumontier, Anna Sànchez Vidal, Miquel Canals, Serge Heussner

Beached microplastics in the Northwestern Mediterranean Sea

Constant Mel, Kerhervé Philippe, Mino-Vercellio-Verollet Morgan, Dumontier Marc, Sanchez-Vidal Anna, Canals Miquel and Heussner Serge.

Constant Mel (https://orcid.org/0000-0003-4808-4373), Kerhervé Philippe, Mino-Vercellio-Verollet Morgan, Heussner Serge.

Université de Perpignan Via Domitia, Centre de Formation et de Recherche sur les Environnements Méditerranéens, UMR 5110, 52 Avenue Paul Alduy, F-66860 Perpignan cedex, FRANCE.

CNRS, Centre de Formation et de Recherche sur les Environnements Méditerranéens, UMR 5110, 52 Avenue Paul Alduy, F-66860 Perpignan cedex, FRANCE.

Dumontier Marc.

Parc Naturel Marin du Golfe du Lion (PNMGdL), Agence Française pour la Biodiversité, 2 impasse Charlemagne, 66 700 Argelès-sur-Mer, France.

Sanchez-Vidal Anna, Canals Miquel.

Universitat de Barcelona, GRC Geociències Marines, Departament de Dinàmica de la Terra i de l'Oceà, Facultat de Ciències de la Terra, Universitat de Barcelona, C/ Martí Franquès s/n, 08028 Barcelona, Spain.

Contact: mel.constant@lilo.org, kerherve@univ-perp.fr.

Key words: microplastics, Mediterranean Sea, Gulf of Lion, micro-tidal system, beach.

Abstract

Microplastics are small (< 5mm) fragments of plastic debris that are ubiquitous in coastal areas and in open ocean. We have investigated the occurrence and composition of microplastics in beach sediments from the micro-tidal Northwestern Mediterranean Sea. Samples were collected on two beaches (northern and southern site) of the western Gulf of Lion showing markedly different characteristics. Sampling was performed along depositional lower, mid and upper beaches and repeated after 1 month. Concentrations of microplastics in the northern and southern site were highly variable, ranging from 33 to 798 and from 12 to 187 microplastics per kg of dry sediment, respectively. Highest concentrations were found at three specific locations: nearby a local river mouth, within an accretionary area and in a depositional upper beach. The spatial and temporal distribution of beached microplastics seems to be directly dependent on external forcing such as wind, swell, precipitation, outflow and river mouth proximity.

1. Introduction

Numerous reports qualify anthropogenic litter as a pervasive and persistent global threat to natural environments. Indeed, it occurs in terrestrial (Zubris and Richards, 2005), subterranean (Panno *et al., 2019*), freshwater (Gasperi *et al.*, 2014) and marine ecosystems (Moore *et al*., 2001). Even remote habitats are concerned as shown by the finding of man-made litter in mountain lakes and isolated islands (Free *et al.*, 2014; Lavers and Bond, 2017). Oceans and seas are widely considered as a sink for anthropogenic litter, produced either by terrestrial or marine human activities, which triggers a number of environmental and economic issues. Though floating marine litter can provide habitat and shelter to a variety of organisms it is first and above all a threat for marine life mainly through ingestion and entanglement. Marine litter is also undesirable for humans as it affects local and national economies in terms of environmental pollution, tourist choice for beaches and sea-going recreational activities, or by inducing expensive clean-up costs (Krelling *et al.*, 2017). This pervasive problem should persist in the future even if inputs of new debris would stop now (Barnes *et al.*, 2009).

Plastics represent the largest item category described within beached marine litter, which may reach up to 90% of total debris in some beaches (Laglbauer *et al.*, 2014). Furthermore, the number of plastic pieces drastically increases with decreasing size. Particles smaller than 5 mm, called microplastics (MPs hereafter), can represent more than half of all plastic debris (Munari *et al.*, 2017). MPs can be ingested by small invertebrates and potentially transferred to higher trophic levels through the food web (Farrell and Nelson, 2013). Concern has been even formulated on potential impact on human health since MPs have

been found in seafood, salt and airborne particles (Rochman *et al.,* 2015; Yang *et al.,* 2015; Dris *et al.,* 2016).

In 2008 the European Union launched the Marine Strategy Framework Directive (MSFD), a policy framework aiming to achieve a good environmental status of marine waters. One of the selected criteria relates to marine litter with a particular attention to small plastic particles, which should be monitored within four compartments: along coastlines (shored MPs), at the sea-surface (floating MPs), in marine sediments (settled MPs), and in the biota (ingested MPs). Protocols regarding the quantitative assessment of macrolitter are well established in Europe (OSPAR 2010; Galgani, 2013) and the most recent studies comply with them (Poeta *et al,* 2016; Portman and Brennan, 2017). In contrast, MPs are still studied using a wide range of non-standardized methods and protocols, a situation that does not favor data comparison nor the calculation of budgets.

As a landlocked sea, the Mediterranean Sea is highly exposed to marine litter pollution (Cózar *et al.*, 2015; Deudero and Alomar, 2015; Tubau *et al.,* 2015). This is partly explained by high population densities in many of the Mediterranean watersheds, its appeal as one of the most popular tourist destinations in the world, and also by its semi-enclosed nature favoring litter recirculation and limiting an unrestricted transfer to other ocean areas. Marine litter thus significantly adds to the high anthropogenic pressures threatening the ecosystems of the Mediterranean Sea where at least 134 species are impacted (Deudero and Alomar, 2015).

A number of studies have recently addressed floating MPs in the Mediterranean Sea, and specifically in the Gulf of Lion in its northwestern part (Collignon *et al.*, 2012, 2014; Faure *et*

al., 2015; Pedrotti *et al.*, 2016; Schmidt *et al*., 2017; Constant *et al*., 2018). However, only a few investigations have been conducted on MPs stranded on beaches (Kaberi *et al.,* 2013; Laglbauer *et al.,* 2014; Lots *et al.,* 2017; Munari *et al.,* 2017; Abidli *et al.,* 2018). The MSFD guidance document (Galgani *et al*., 2013) for sampling beached MPs focuses on intertidal sediments and high tide lines. However, in the Mediterranean Sea, which is a microtidal environment, alongshore depositional line marks are not due to tides but to hydrodynamic conditions such as surges and storms. Thus, the first objective of our study was to sample nearby Mediterranean beaches representative of different settings and depositional conditions at high spatial resolution in search for patterns in the quantitative (density) and qualitative (size, shape and polymer composition) distribution, temporal variation and properties of MPs in the 5 mm - 63µm size range. The second objective was to examine the potential role of external forcing such as precipitation, flooding, surging, wind regimes and specific events on the distribution and temporal variation of beached MPs.

2. Materials and Methods

2.1. Study area

The Gulf of Lion is a passive margin covering 11,000 km^2 from Cap Croisette in the northeast to Cap Creus in the southwest (Fig. 1). This river-dominated continental margin is a micro-tidal environment characterized by large supplies of freshwater, sediments, nutrients and contaminants (Durrieu de Madron *et al.,* 2000, 2009; Ludwig *et al.,* 2009; Bouloubassi *et al.,* 2012). The most important river flowing into the Gulf of Lion is the Rhône River that at present is also the highest freshwater input to the Mediterranean Sea

with a mean annual flow rate of 1700 m^3 s^{-1} and yearly floods higher than 5000 m^3 s^{-1} (Maillet *et al.,* 2006, Ludwig *et al.,* 2009). Inputs of particulate matter from the Rhône River represents on average 80 to 95% of the total inputs to the gulf (Bourrin *et al.,* 2006; Sadaoui *et al.,* 2016). Its mouth is located 180 km northeast from our sampling area in the southwestern Gulf of Lion. Suspended sediments at sea are mainly carried by the Northern Current and generally follow a south-southwest direction as far as the southwestern end of the gulf (Arnau *et al.,* 2004).

Several small coastal rivers, as the Têt River, discharge also freshwater, sediments and contaminants along the central and western part of the gulf (Sadaoui *et al.,* 2016) but with a lower contribution than the Rhône River. These coastal rivers are characterized by small watersheds (< 5,000 km^2) and a highly variable discharge regime governed by episodic flood events. Indeed, their contribution to sediment inputs into the Gulf of Lion reaches a long-term average of about 5% of the total amount of riverine sediments, except in some particular years with frequent flash-floods (up to 90% and 27% of the monthly and yearly sediment discharge respectively). The 116 km long Têt River, a typical Mediterranean coastal river with its source in the Pyrénées mountain range and a mean slope of 12.1°, dominates continental inputs to the study area (Fig. 1). With a long-term annual average discharge of 10 m^3 s^{-1} this river, as most Mediterranean coastal rivers, shows long periods of low-water stages (<3 m^3 s^{-1}) interrupted by yearly flash-flood events (>100 m^3 s^{-1}) peaking at 1.800 m^3 s^{-1} (Serrat *et. al.*, 2001). The lower course of the Têt River flows across a 600 km^2 agricultural alluvial plain. Perpignan is the main town there with around 150,000 inhabitants. The urban wastewater treatment plant of Perpignan has a direct effect on the

chemistry of the Têt River, by increasing nutrients and pollutants (Garcia-Esteves *et al.*, 2007; Reoyo-Prats *et al.,* 2017).

Two markedly different beaches, both in terms of setting and sedimentary conditions, have been selected (Table 1). Both beaches are located 25 km (straight) and 35 km (alongshore) apart. These beaches are ”La Crouste” Beach, to the north, (hereafter also called “northern site”) nearby the Têt River outlet, and “Fourat Beach” (hereafter “southern site”) (Fig. 1). The northern site is bordered at its southern end by the Têt River mouth and at its northern end by a man-made jetty (Fig. 2A). The combined effects of the jetty and a northward alongshore current lead to preferential sediment accumulation at the northern part of the beach. At its innermost, upper part, the beach is bounded by dune vegetation. The southern site backshore is bounded by natural boulders and a concrete wall (Figs. 2E and F). Onshore winds and associated waves induce a southward alongshore current (Brunel *et al.,* 2014), and sediment accumulates mainly at the southern end of the beach. This site may receive sediments and plastic materials used in the surrounding terraced vineyards through a small, 0.6 km^2 dry creek during rainfall events. Both sites are affected by “Tramontane”, a strong, persistent and dry NNW wind with gusts often exceeding 100 $km.h^{-1}$. They are also affected by eastern sea storms associated to humid winds and precipitation (Sanchez-Vidal *et al.,* 2012). As for most Mediterranean beaches, they are both popular leisure spots in summer. No activities related to plastic production or treatment have been identified around these study sites.

2.2. Sample collection

Given the microtidal regime of most of the Mediterranean Sea, deposit lines on beaches are mainly dependent on surges due to atmospheric conditions (pressure and wind) and on wave height. Three debris deposit lines at different heights can be distinguished most of the time on the shores of the Gulf of Lion (Figs. 2B and F). The first deposit line, at the lower beach, is freshly produced and generally wet. The second one, close to the beach mid-height, is composed of dried up materials stranded during gales. The third one, at the upper beach, corresponds to materials accumulated during stormy conditions and subsequently trapped in the backshore. At the northern site, trapping is due to the dune vegetation, while at the southern site it is favored by the concrete wall and beach-end boulders. At the northern site, the mid-beach line was associated to a berm crest (Fig. 2D). Sampling was performed along the 3 deposit lines named from here onwards “lower”, “mid” and “upper”, at the crossing of four cross-beach transects termed “north”, “mid-north”, “mid-south” and “south” (Figs. 2C, D, G, and H).

In total, 12 samples were collected on each site using a 0.5 x 0.5 m wood quadrat. The top first centimeter of sand was sampled with a steel trowel and sieved through an 8 mm steel sieve placed on top of a metallic funnel to avoid obstruction of the funnel by plant residues and/or gravels. The <8 mm fraction was funneled into glass bottles. This sampling was repeated twice at each site: on March 2 and March 30, 2016 for the northern site, and on February 22 and March 30, 2016 for the southern site.

2.3. Sample treatment

Contamination of samples was minimized by wearing laboratory cotton coats and by using glass or steel equipment and tools, rinsed with MilliQ® water and wrapped in aluminium foils. Back in the laboratory, samples were dried at 50°C during one week and weighed. Samples were sieved through a column of sieves (5, 2.5, 1 mm; 500, 315, 63 µm) placed in a mechanical shaker. Parts <63 µm were discarded, as the available equipment did not allow accurate measurements of such small particles. The protocol for MP density-based extraction from sediments provided by Thompson (2004) was adapted to our samples: 550 mL of concentrated saline solution (density 1.2 g mL^{-1}) were added to 500 g of sorted sand in a boiling flask and hand-stirred for two minutes. After 30 minutes the supernatant was filtered on GF/F Whatman filters (47mm diameter; 0.7µm porosity). This extraction procedure (stirring and decantation) was repeated until all floating particles were recovered. At least 3 repetitions were performed, and four repetitions were generally sufficient to reach full extraction. Filters were dried at 50ºC overnight and then examined under a Wild Heerbrugg dissecting stereo-microscope (6 x, 12 x, 25 x and 50 x magnification). Several contamination control filters were simultaneously performed as blanks with the same concentrated saline solution. Particles were separated into 5 shape categories: fibers (including filaments and fishing line fragments; Figs. 3A and B), fragments (items with a three-dimensional shape; Fig. 3C), micro-beads (solid spheres; Fig. 3C), films (items with a two-dimensional shape; Fig. 3C), and foams (pieces or spheres with a spongy, soft structure; Fig. 3C). These categories have been used in previous studies (Kaberi *et al,* 2013; Faure *et al.,* 2015; Abidli *et al.,* 2018).

2.4. Polymer analysis with FTIR spectroscopy

Five items for each size fraction (including the >5 mm fraction) and shape category (except beads) were randomly selected at each site and analyzed to determine their plastic nature and where appropriate their polymeric composition (Löder and Gerdts, 2015). A total of 40 fibers, 60 fragments, 60 films, 60 foams and 4 beads were examined (fibers were only present inside four size classes). MPs were analyzed with a Perkin Elmer Frontier FTIR spectrometer, and fibers, due to their small volumes, were analyzed with a microscope IR-Plan Spectra Tech coupled to a Bomem ABB FTLA FTIR spectrometer.

The identification of each polymer was performed by comparison with a self-collected spectrum database including polyethylene (PE), polypropylene (PP), polyamide (PA), polyvinyl chloride (PVC), polystyrene (PS), poly(ethylene-vinyl acetate) (PEVA), poly(ethylene terephthalate) (PET), polyester (PES), polyurethane (PUT), acrylic (A) and some non plastic materials such as cotton, wool, wood, paper, calcium carbonate, talcum powder and plant fibers. Only polymers reaching at least 70% of similarity with reference spectra were accepted, according to the suggestion of Thompson *et al.* (2004). The rejected items were counted in the unidentified category.

2.5. Data analysis

FTIR analysis was used to correct the initial sorting and accurately determine true MPs in our samples. For each shape category, an identified plastic ratio was accordingly applied. This ratio was calculated by dividing the number of true particles, with a “plastic spectra”, by the total number of sorted items and visually described as “potential plastics”. All MP contents and relative contents of shapes given in the following text, figures and tables are

based on identified MPs. Mean values are provided ± 1 standard error. Finally, concentrations of MPs were estimated by dividing the corrected numbers of identified plastic items by the size of the surface sampled on the beach (items per m^{-2}) or by the weight of the dry sand sampled (items per kg^{-1}). Statistical analyses were performed using R software (R Core Team, 2018; caption package "captioner": Alathea, 2015; manuscript package "rmarkdown": Allaire *et al.*, 2018; data manipulation package "dplyr": Wickham *et al.*, 2017; graphical package "ggpubr": Kassambara, 2017; graphical package "scales": Wickham, 2017). As normality of distributions was never observed (Shapiro-Wilk test), three non-parametric tests were used: the Wilcoxon-Man-Whitney test to compare means of two groups; the Scheirer-Ray-Hare test to compare variances with two factors and the interaction among factors; and the post hoc Dunn's test to compare differences of all possible pairs and pinpoint which specific means are significantly different from the others.

3. Results

3.1. MPs spatial distribution

A total of 15,664 particles have been sorted from the 48 samples collected on the two beaches and at the two periods (Table 2). After FTIR analysis, it appeared that only 45% of them were really plastics. Mean concentration of MPs was 166 ± 205 items kg^{-1} for the northern site (range 33 to 798 items kg^{-1}) and 58 ± 53 items kg^{-1} for the southern site (range 12 to 187 items kg^{-1}).

Both sites significantly differ regarding MP concentrations (p-value <0.01; Fig. 4A). Though concentrations of MPs changed by a factor up to three for some limited cross-beach

transects between the first and the second period no statistically significant differences were found between the two sampling periods at each site (northern site: p-value = 0.79; southern site: p-value = 0.47; Fig. 4A). The data were therefore consequently pooled to gain readability (Table 3; Figs 5 and 6).

The range of MP concentrations measured in the northern site spanned over an order of magnitude, from a minimum of 33 to a maximum of 798 items kg^{-1} (Table 2). Concentrations at the two extreme cross-beach transects (North and South) were quite heterogeneous, while middle cross-beach transects (Mid-North and Mid-South) showed low and stable values. Highest mean concentrations (>300 items kg^{-1}), significantly different from the other "baseline" samples (Fig. 4D), were located at the medium and high alongshore transects along the "North" and "South" cross-beach transects (Fig. 5). The 3 major impacted zones ("High Concentration Zones"), represented half (52%) of the total number of MPs found in the 24 samples collected on that beach. Finally, MP concentrations did not significantly differ between alongshore transects (p-value = 0.16; Fig. 4B), cross-beach transects (p-value = 0.06; Fig. 4C) or the interactions among cross-beach transects and alongshore transects (p-value = 0.65).

MP concentrations measured at the southern site ranged from a low of 12 to a high of 187 items kg^{-1} (Table 2). They were more stable than in the northern site. The major, obvious outcome of the survey there was the strong difference in concentrations between alongshore transects (p-value <0.01; Fig. 4B). The highest concentrations were all located in the high deposition line (Fig. 6). With an overall mean concentration of 115 items kg^{-1}, compared to the overall means of 30 items kg^{-1} for the other two alongshore transects, the

high line concentrated more than half (57%) of the total MPs in that area (Fig. 6). Though differences between cross-beach transects were not significant (p-value = 0.15; Table 3), it seems that an increase of MP concentrations occurred along the beach from North to South, i.e. in the direction of the alongshore current, especially in the high alongshore transect. Again, the interaction among cross-beach transects and alongshore transects was not significant (p-value = 0.97). MPs distribution throughout the beach sampled at the end of February exhibited a very similar spatial pattern than the one observed at the end of March (data not shown).

3.2. Shape and polymers

Due to the high number of shape categories considered, data from the different samples were pooled within each study site. Fibers were the most abundant shape found at both beaches (northern site: 59% ; southern site : 77%; Fig. 7), followed by fragments (northern site: 25%; southern site : 17%) and foams (northern site: 12%; southern site : 5%). Films were less represented (<5%) and micro-beads were negligible (<1%). Some changes in the shape distributions occurred between the two sampling periods. In the northern site, fragments, films, foams and beads were mainly present during the first sampling period, whereas fibers were mainly present during the second sampling period. In the southern site, beads were only present during the first sampling period, fibers and films were equally present in both sampling periods, and fragments and foams were mainly present during the second sampling period.

Our FTIR results confirmed the necessity of performing plastic polymer analysis for correcting the data. Indeed, we found that less than half of binocular-sorted items (45%)

were plastic. The overall percentage was only 37% for fibers, which accounted for 63% of all the plastic items sampled during this study. Such a low percentage of plastic likely relates to the difficulty in discriminating plastic fibers from cotton and plant fibers with a binocular or a dissecting stereo-microscope. Among the plastic fibers, polyester, acrylic and polyacrylamide were the three most abundant polymers. Fragments were also characterized by a low percentage of plastic. Only half (50%) of the sorted fragments were really plastic polymers, mostly composed of polypropylene (17%), polyethylene (15%) and polystyrene (9%). The presence of calcium carbonate and cellulose identified by FTIR spectra suggests that they have been probably mistaken for shells and plant debris. The identified plastic rate reaches 67% for films with the same major polymers than those in fragments: polypropylene (37%), polyethylene (18%) and polystyrene (10%). A low error rate was measured for foams, probably due to their larger size and particular texture, as 81% of foam items were really plastics, predominantly and logically made of polystyrene (74%). Sorted beads were only plastic items made of polyethylene (100%).

3.3. Size

Regarding MP distributions within the sand size classes obtained by sieving, no major differences were observed between the northern and southern sites (Fig. 8). The former had higher MP concentrations within each size class. MPs within the smallest sand fraction (<0.5 mm) were mainly fibers, fragments and films, whereas in the largest ones (>2.5 mm) foams predominated and fibers prevailed in the other fractions. Fibers and foams showed skewed unimodal distributions towards larger size classes. Most of the fibers appeared within the median sand size classes (0.5-2.5 mm) and only a few fibers were found within

the >2.5 mm size classes. Foams belonged to the largest sand size classes (1-5 mm) with high variations between samples from the northern site. Fragments and films were more evenly distributed in the different classes with higher concentrations within the lowest sand size, especially in the northern site where the lowest sand size class (0.063-0.315 mm) had the highest fragment and film concentrations. Beads only belonged to the upper size classes (> 1 mm).

3.4. Meteorological and hydrological context

Two meteo-hydrological periods can be distinguished: a first period from October 2015 to the end of February 2016 (the first sampling date of the southern site) and a second period until the last sampling date at the end of March 2016 (Fig. 9). The first period was mainly characterized by a winter storm associated to a short but intense rainfall event (36 mm of rain fell within a few hours; Fig. 9A) at the beginning of November 2016 that resulted in a peak of the Têt River flow (daily mean peak of 150 m^3 s^{-1}; Fig. 9D), just below the flood threshold (170 m^3 s^{-1}, biennial return period). Simultaneously, south to southeasterly winds at around 13 m s^{-1} (Fig. 9C) generated the highest swells (up to 5 m height; Fig. 9B) and a consequent storm surge on the shoreline. From this seasonal event to the first sampling date (February 22, 2016) no particular meteorological or hydrological events happened at the local scale. The Têt River was characterized by a long period of low water stage (< 5 m^3 s^{-1}) and swells and winds did not exceed 3 m and 16 m s^{-1}, respectively. The continental, dry and intense wind ("Tramontane") blew often during this interval. The second period was characterized by an important rainfall event (up to 62 mm) generating only a small Têt

River flow peak (12 m^3 s^{-1}) that occurred between the two first sampling dates, at the southern (February 22, 2016) and northern (March 2, 2016) sites. This second period was further characterized by strong SSE winds (up to 13 m s^{-1}) and high swells (up to 4 m). Then, the wind turned mainly northwest and no significant rainfalls or storms were recorded. The Rhône River did not experience any flood (>3,500 m^3 s^{-1}; Fig. 9D) during this 6-month period. Its flow rate peaked three times in 2016 over 3,200 m^3 s^{-1} (peak at 3,850 m^3 s^{-1} February 2016), but they were far from reaching the flood biennial return frequency of 5,700 m^3 s^{-1}.

4. Discussion

4.1. Levels of MP pollution on NW Mediterranean beaches

MP concentrations found along two French Mediterranean beaches varied within the range of MP concentrations measured so far in various locations along the Mediterranean coast (Table 4). Kaberi *et al*., (2013) and Munari *et al*. (2017) found low concentrations that may be explained, at least for the former, by their focus on only larger MPs (1-4mm) and thus the lack of significant amounts of fibers. Fibers accounted, on average, for 63% of all MP items collected in our study. They predominated also on Slovenian and Tunisian beaches (Laglbauer *et al.*, 2014; Abidli *et al.,* 2018) and reached up to 99% of MPs on various Mediterranean beaches (Lots *et al.*, 2017). Synthetic fibers in oceans and beaches can originate from clothes (Napper and Thompson 2016) but also from fishing gears (Claessens *et al.*, 2011; Lots *et al.*, 2017). Fiber textiles can break due to pilling in laundry washing machine and reach wastewater treatment plants (WWTP). Napper and Thompson (2016) estimated at up to 700,000 the number of fibers produced during a single wash. Although

WWTP strongly reduce MPs in wastewaters (up to 98%, Murphy et al. 2016), the treated effluent flowing into rivers or seas still contain significant amounts of MPs. Moreover, synthetic fibers have been also found in sewage sludges used for agricultural fertilization (Zubris and Richards, 2005), representing thus a supplementary source to agricultural watersheds such as the Têt River. Lots *et al.*, (2017) also described the so far highest Mediterranean hotspot of stranded MPs with concentrations up to 1,512 items kg^{-1}, a value about twice the highest MP concentration observed in our study (798 items kg^{-1}). According to the authors this hotspot may be explained by the geographical position of the site, situated between the mouths of two rivers. Considering that sample collection and treatment, especially visual sorting and FTIR validation, potentially create noticeable differences between studies, even such concentrations should be considered, in a first approximation, as similar. Our highest MP concentrations found in the northern site thus probably lie close to the upper limit of the contamination range observed so far on Mediterranean beaches. The Mediterranean Sea has been identified as a region of particularly high floating plastic concentrations in comparison to the range measured for the global ocean (Cózar *et al.*, 2015). However, our results (Table 2) and those obtained by previous studies (Table 4) indicate that this situation is not as dramatic for MPs stranded on beaches elsewhere. They are indeed much lower than the 250,000 items m^{-2} found in a Hong-Kong beach (Fok and Cheung, 2015) or 24,000 items m^{-2} found in Hawaï (McDermid and McMullen, 2004). More studies are needed to determine if such high concentrations exist in the Mediterranean Sea, and particularly along the south Mediterranean coast where recent models of plastic distribution predict high beaching (Mansui *et al.*, 2015).

4.2. Small scale spatial variability in the distribution of MPs

The two study sites have been selected to represent markedly different environmental settings, within a limited geographical area of the Northwestern Mediterranean Sea: a sandy beach bordered by a river mouth and thus directly affected by river litter inputs and a sandy beach located on a rocky coast supposed to be less affected by direct anthropogenic pressures (rivers and anthropized watershed). Despite some similarities in both beaches, such as the presence of high concentration zones (HCZ), the low and quite constant MP concentrations in the lower alongshore transects, or the predominance of fibers (overall mean of 63% for both beaches), the distribution of the concentration of MP at a small scale was quite different between the northern and the southern sites.

The northern site shows the highest MP concentrations (mean value up to 798 items kg^{-1} and maximum of 4,654 items m^{-2}), about three times higher than those found in the southern site. This quantitative difference is likely due to the close proximity of the Têt River mouth at the southern end of the site. This small and typical coastal Mediterranean river drains a small watershed, mainly wild in its upper part but highly anthropized downstream. The riverine MP content ranges between 1 and 2 items m^{-3} (Constant, unpublished results), a concentration 10 times higher than that in surficial coastal waters a few kilometers off the river mouth (Constant *et al.*, 2018). These values suggest that MPs delivered by the Têt River and transported by the northward alongshore drift can be an important if not the major direct source of plastics to this beach. Such a direct connexion has been already described by Munari *et al.* (2017) for a beach located next to the Po River. Mean MP concentrations in the northern site were similar between the two sampling

periods (182 and 150 items kg^{-1}) but the HCZ moved from a position close to the river mouth at the upper deposition line to the mid-deposition line of the opposite and northernmost cross-beach transect within 1 month. The limited spatial extension of the HCZs is also noteworthy as the high concentrations quickly dropped at a distance of a few tens of meters around. The northern HCZ observed during the second sampling period was located within a beach accretion area generated by a jetty. The medium deposition line of this northernmost cross-beach transect was more impacted by MPs than the high and low alongshore transects likely because the presence of a slight depression on the bern at this line. The high deposition line is probably not a final accumulation zone because previous extensive storm surges washed this flat place and moved the debris towards the vegetated area bordering the beach.

The southern site is not directly affected by close river inputs or urbanized areas. Consequently it receives less MPs than the northern site. MP concentrations there are highly dependent on the sampled deposit line, and the high deposit line may be qualified as an HCZ. The presence of a concrete wall and boulders along the upper part of the beach obviously prevents the migration of litter beyond that physical barrier during surge periods and concentrates all types and sizes of floating debris there. MPs found on this site are probably originating from floating MPs drifting with the general circulation. The degradation and fragmentation processes of large plastic debris deposited on the beach can be another source, but probably limited since sporadic cleaning operations are performed during the summer season, limiting the residence time of large debris to less than a year. Moreover, Hinata *et al.* (2017) estimated that MPs have shorter residence times on beaches than large plastic litter. They hypothesized that macrolitter is pushed towards the

backshore while micro- and mesolitter are backwashed to the sea by waves. Our study therefore points out that in the micro-tidal Mediterranean Sea the small scale spatial distribution of MPs is highly heterogeneous and strongly dependent on the morphological and environmental settings of the studied beaches. Among the few studies carried out at a high spatial resolution, Dekiff *et al.* (2014) found that MPs were rather homogeneously distributed within a beach of Norderney Island, a meso-tidal region of the North Sea, whereas Turra *et al.* (2014) showed a high spatial variability in the MP distribution within Brazilian beaches.

4.3. External forcing of MP distribution on NW Mediterranean beaches

Local parameters such as swell height, wind, precipitation and river flow affect marine litter transport and may explain MP distributions and the presence of HCZs on beaches (Galgani *et al.,* 2015). We hypothesize that most of MPs stranded on the southern site and sampled in February are MPs washed away from the urbanized watershed and discharged by local rivers such as the Têt River in November, during a flood associated with intense southeastern winds and surge waves. This November storm and the related surge accounted also for the location of HCZs always within the high deposit line of the southern site. In addition, the MP accumulation towards the southern part of this beach is explained by the alongshore current prevailing in this area (Fig. 2). Another important feature of the southern site is the relative similarity of MP distributions throughout the beach between the two sampling periods (40 days). The remote location of this beach from the urbanized plain and its rivers, as well as the lack of extreme meteorological events during this interval may explain this small scale stability.

MP inputs to the northern site are more difficult to untangle. Besides the November storm, one must also consider the intense rainfall of February 2016 (60 mm), a few days before sampling. Precipitation was probably sufficient for washing away all plastic litter from local watersheds and concentrating them into streams and rivers. As the rainfall was spread over the day, the daily flow rate of the Têt River did not exceed 10 m^3 s^{-1}, but the related southeastern winds and swell heights were probably sufficient to ground large amounts of litter and MPs at the proximity of the Têt mouth and at the upper beach. The second sampling date (end of March 2016) was mainly preceded by a period of northwestern winds, low water stages and swell heights. Such a continental wind can blow the stranded litter offshore (Galgani *et al.,* 2000) and thus erode the HCZ previously shaped close to the Têt river mouth. It is interesting to note that the HCZs on the northern site have been fully modified in three weeks. The new HCZ observed at its northern part may have been formed by the northward alongshore current. The lack of stormy sea during these 3 weeks explains the MP deposition at mid-beach level.

The contribution of the Rhône River to MP inputs into the Gulf of Lion and onto these local beaches cannot be ruled out as the southern general circulation combined with eastern winds and waves may beach some floating MPs. The Rhône River is currently the largest Mediterranean river in terms of freshwater and sediment discharges. Sadaoui *et al.* (2016) found that coastal rivers contribute on average only to slightly more than 5% of long-term sediment inputs to the Gulf of Lion and the Rhône River for 95%. The Rhône River did not experience any flood during the 6 months preceding the first sampling. Moreover, the periods of outflow peaks coincided with periods of low swell heights that cannot explain the HCZs along the upper part of both beaches.

Some changes of shape assemblages due to external forcing have been noticed by Browne *et al.* (2010), who observed denser MPs in UK down-wind beaches when compared with up-wind beaches, and by Fazey and Ryan (2016) who observed along the South African coast an increasing shift in the shape distribution with increasing distance from a potential terrestrial source. No obvious relation was found in our study. Shape assemblages were quite similar between the two sampling sites and the two sampling periods. The major change observed was between the HCZs of the two sampling periods at the northern site. At the first sampling period, fragments, foams and fibers were present with similar proportions in the HCZs, while at the second sampling period fibers prevailed. This difference may be due to different transport pathways of different sources of MPs. The combination of precipitation and stormy sea before the first sampling period could have brought high amounts of fragments and foams close to the Têt mouth, whereas deposition of MPs with a majority of fibers at the HCZ of the second sampling period could have resulted from atmospheric fallout (Dris *et al.,* 2016), input of wastewater treatment plant effluent in the river (Mason *et al.*, 2016) or marine activities (Claessens *et al.*, 2011).

5. Conclusion

This study on beached MPs innovates in performing a high-resolution spatial survey on the micro-tidal Mediterranean Sea, moreover with high methodological concerns. A number of conclusions may be drawn from this study on the spatial distribution of MPs on two markedly different beaches from the Gulf of Lion (NW Mediterranean Sea). Some pertain to the quality assessment of MPs and some concern the level of contamination of these beaches and the role of external forcing, such as rainfall, river flow, wind and swell height on MP distribution.

(1) Including fibers among the MP shapes considered is crucial for any study dealing with beached MPs. Though sorting fibers is a time-consuming operation that may be furthermore affected by contamination during sample treatment, it appears as being excessively important since fibers represented an overall 63% of our 15,664 sorted items.

(2) The analytical confirmation (and identification) of plastic polymers is critical to accurately quantify and qualify MPs. Analyses by FTIR spectrometers of more than 200 suspected MPs revealed that only 45% of them were really plastic polymers. This analytical step is particularly relevant when samples are mainly composed of fibers, which were minorly (37%) made of plastic in this study.

(3) Both NW Mediterranean beaches were affected by MP contamination but their concentrations (means: 166 ± 205 items kg^{-1} and 58 ± 53 items kg^{-1}) varied within the range of concentrations observed so far along the Mediterranean coast. Highest concentrations (up to 800 items kg^{-1} or 4,650 items m^{-2}) are close to the highest

Mediterranean beach concentrations (1,512 items kg^{-1}; Lots et al., 2017) but far from the world most polluted beaches (250,000 items m^{-2}; Fok and Cheung, 2015).

(4) Our high-resolution study highlights the complexity of MP distribution on beaches. The spatial distribution can be strongly heterogeneous at small scale and can change within a 1-month interval. MP concentrations quickly dropped around HCZ over a distance of only a few tens of meters. Therefore, stranded MP concentrations depend on the sampling strategy, especially along the Mediterranean micro-tidal coast, where the upper deposition line seems to concentrate and to retain MPs.

(5) The geographical context of the beach and the proximity of potential MP sources (e.g. river, urban area) seem to influence the level of contamination by MPs, whereas the morphological setting and external forcing may affect both the quantity and the type of MPs at a small spatial scale.

6. Acknowledgement

We acknowledge the "Ecole Doctorale ED305" from the University of Perpignan Via Domitia for funding the PhD grant of Mel Constant and the “Parc naturel marin du golfe du Lion” for the Master grant of Morgan Mino-Vercellio-Verollet. We thank Núria Ferrer from the “Centres Científics i Tecnològics” of the University of Barcelona for her technical support during FTIR analyses. We are also grateful to the “Centre d'études et d'expertise sur les risques, l'environnement, la mobilité et l'aménagement” (CEREMA) for providing us swell data, “Météo–France” for the access to weather data and the Banque Hydro hosted by the “French Ministère de l'Environnement et du Développement durable” for hydrological data. This research has also been supported by a Catalan Government Grups de Recerca Consolidats grant (2014 SGR 1068).

7. References

Abidli, S., Antunes, J.C., Ferreira, J.L., Lahbib, Y., Sobral, P., Trigui El Menif, N., 2018. Microplastics in sediments from the littoral zone of the north Tunisian coast (Mediterranean Sea). Estuarine, Coastal and Shelf Science 205, 1–9. https://doi.org/10.1016/j.ecss.2018.03.006

Alathea, L., 2015. Captioner: Numbers figures and creates simple captions. https://CRAN.R-project.org/package=captioner

Allaire, J., Xie, Y., McPherson, J., Luraschi, J., Ushey, K., Atkins, A., Wickham, H., Cheng, J., Chang, W., 2018. Rmarkdown: Dynamic documents for R. https://CRAN.R-project.org/package=rmarkdown

Arnau, P., Liquete, C., Canals, M., 2004. River Mouth Plume Events and Their Dispersal in the Northwestern Mediterranean Sea. Oceanography 17, 22–31. https://doi.org/10.5670/oceanog.2004.27

Barnes, D.K.A., Galgani, F., Thompson, R.C., Barlaz, M., 2009. Accumulation and fragmentation of plastic debris in global environments. Philosophical Transactions of the

Royal Society B: Biological Sciences 364, 1985–1998. https://doi.org/10.1098/rstb.2008.0205

Bouloubassi, I., Roussiez, V., Azzoug, M., Lorre, A., 2012. Sources, dispersal pathways and mass budget of sedimentary polycyclic aromatic hydrocarbons (PAH) in the NW Mediterranean margin, Gulf of Lions. Marine Chemistry 142-144, 18–28. https://doi.org/10.1016/j.marchem.2012.07.003

Bourrin, F., De Madron, X. D., Ludwig, W., 2006. Contribution to the study of coastal rivers and associated prodeltas to sediment supply in the Gulf of Lions (NW Mediterranean Sea). Vie et Milieu, 56(4), 307-314.

Browne, M.A., Galloway, T.S., Thompson, R.C., 2010. Spatial Patterns of Plastic Debris along Estuarine Shorelines. Environ. Sci. Technol. 44, 3404–3409. https://doi.org/10.1021/es903784e

Brunel, C., Certain, R., Sabatier, F., Robin, N., Barusseau, J.P., Aleman, N., Raynal, O., 2014. 20th century sediment budget trends on the Western Gulf of Lions shoreface (France): An application of an integrated method for the study of sediment coastal reservoirs. Geomorphology 204, 625–637. https://doi.org/10.1016/j.geomorph.2013.09.009

CANDHIS, 2016. Centre d'Archivage National de Données de Houle In–Situ, swell in–situ data bank hosted at the french Center for Maritime and Fluvial Technical Studies. http://candhis.cetmef.developpement–durable.gouv.fr (Consulted in April 2016).

Claessens, M., De Meester, S., Van Landuyt, L., De Clerck, K., Janssen, C.R., 2011. Occurrence and distribution of microplastics in marine sediments along the belgian coast. Marine Pollution Bulletin 62, 2199–2204. https://doi.org/10.1016/j.marpolbul.2011.06.030

Collignon, A., Hecq, J.-H., Glagani, F., Voisin, P., Collard, F., Goffart, A., 2012. Neustonic microplastic and zooplankton in the North Western Mediterranean Sea. Marine Pollution Bulletin 64, 861–864. https://doi.org/10.1016/j.marpolbul.2012.01.011

Collignon, A., Hecq, J.-H., Galgani, F., Collard, F., Goffart, A., 2014. Annual variation in neustonic micro- and meso-plastic particles and zooplankton in the Bay of Calvi (Mediterranean–Corsica). Marine Pollution Bulletin 79, 293–298. https://doi.org/10.1016/j.marpolbul.2013.11.023

Constant, M., Kerhervé, P., Sola, J., Sanchez-Vidal, A., Canals, M., Heussner, S., 2018. Floating Microplastics in the Northwestern Mediterranean Sea: Temporal and Spatial Heterogeneities, in: Cocca, M., Di Pace, E., Errico, M.E., Gentile, G., Montarsolo, A., Mossotti, R. (Eds.), Proceedings of the International Conference on Microplastic Pollution in the Mediterranean Sea. Springer International Publishing, Cham, pp. 9–15. https://doi.org/10.1007/978-3-319-71279-6_2

Cózar, A., Sanz-Martín, M., Martí, E., González-Gordillo, J.I., Ubeda, B., Gálvez, J.Á., Irigoien, X., Duarte, C.M., 2015. Plastic accumulation in the Mediterranean Sea. PLoS One 10, e0121762.

Dekiff, J.H., Remy, D., Klasmeier, J., Fries, E., 2014. Occurrence and spatial distribution of microplastics in sediments from Norderney. Environmental Pollution 186, 248–256. https://doi.org/10.1016/j.envpol.2013.11.019

Deudero, S., Alomar, C., 2015. Mediterranean marine biodiversity under threat: Reviewing influence of marine litter on species. Marine Pollution Bulletin 98, 58–68. https://doi.org/10.1016/j.marpolbul.2015.07.012

Dris, R., Gasperi, J., Saad, M., Mirande, C., Tassin, B., 2016. Synthetic fibers in atmospheric fallout: A source of microplastics in the environment? Marine pollution bulletin 104, 290–293. https://doi.org/10.1016/j.marpolbul.2016.01.006

Durrieu de madron, X., Abassi, A., Heussner, S., Monaco, A., Aloisi, J.C., Radakovitch, O., Giresse, P., Buscail, R., Kerhervé, P., 2000. Particulate matter and organic carbon budgets for the Gulf of Lions (NW Mediterranean). Oceanologica Acta 23, 717–730. https://doi.org/10.1016/S0399-1784(00)00119-5

Durrieu de Madron X., W. Ludwig, G. Civitarese, M. Gacic, M. Ribera d'Alcalà, P. Raimbault, E. Krasakopoulou, C. Goyet (2009). Shelf-slope nutrients and carbon fluxes in the mediterranean Sea. In "Carbon and nutrient fluxes in continental margins. A global synthesis", Editors: K.K. Liu, L. Atkinson, R. Quinones, L. Talaue-McManus, Global Change - The IGBP Series, Springer-Verlag, XII, pp 364-383

Faure, F., Saini, C., Potter, G., Galgani, F., Alencastro, L.F. de, Hagmann, P., 2015. An evaluation of surface micro- and mesoplastic pollution in pelagic ecosystems of the Western Mediterranean Sea. Environmental Science and Pollution Research 22, 12190–12197. https://doi.org/10.1007/s11356-015-4453-3

Farrell, P., Nelson, K., 2013. Trophic level transfer of microplastic: Mytilus edulis (L.) to Carcinus maenas (L.). Environmental Pollution 177, 1–3. https://doi.org/10.1016/j.envpol.2013.01.046

Fazey, F.M.C., Ryan, P.G., 2016. Debris size and buoyancy influence the dispersal distance of stranded litter. Marine Pollution Bulletin 110, 371–377. https://doi.org/10.1016/j.marpolbul.2016.06.039

Fok, L., Cheung, P., 2015. Hong Kong at the Pearl River Estuary: A hotspot of microplastic pollution. Marine Pollution Bulletin 99, 112–118. https://doi.org/10.1016/j.marpolbul.2015.07.050

Free, C.M., Jensen, O.P., Mason, S.A., Eriksen, M., Williamson, N.J., Boldgiv, B., 2014. High-levels of microplastic pollution in a large, remote, mountain lake. MARINE POLLUTION BULLETIN 85, 156–163. https://doi.org/10.1016/j.marpolbul.2014.06.001

Galgani, F., Leaute, J., Moguedet, P., Souplet, A., Verin, Y., Carpentier, A., Goraguer, H., Latrouite, D., Andral, B., Cadiou, Y., Mahe, J., Poulard, J., Nerisson, P., 2000. Litter on the sea floor along european coasts. Marine Pollution Bulletin 40, 516–527. https://doi.org/https://doi.org/10.1016/S0025-326X(99)00234-9

Galgani, F., Hanke, G., Werner, S., De Vrees, L., 2013. Marine litter within the european marine strategy framework directive. ICES Journal of Marine Science 70, 1055–1064. https://doi.org/10.1093/icesjms/fst122

Galgani, F., Hanke, G., Maes, T., 2015. Global distribution, composition and abundance of marine litter, in: Marine Anthropogenic Litter. Springer, pp. 29–56. https://doi.org/10.1007/978-3-319-16510-3_2

Garcia-Esteves, J., Ludwig, W., Kerhervé, P., Probst, J.-L., Lespinas, F., 2007. Predicting the impact of land use on the major element and nutrient fluxes in coastal Mediterranean rivers: The case of the Têt River (Southern France). Applied Geochemistry 22, 230–248. https://doi.org/10.1016/j.apgeochem.2006.09.013

Gasperi, J., Dris, R., Bonin, T., Rocher, V., Tassin, B., 2014. Assessment of floating plastic debris in surface water along the Seine River. Environmental Pollution 195, 163–166. https://doi.org/10.1016/j.envpol.2014.09.001

Hinata, H., Mori, K., Ohno, K., Miyao, Y., Kataoka, T., 2017. An estimation of the average residence times and onshore-offshore diffusivities of beached microplastics based on the population decay of tagged meso- and macrolitter. Marine Pollution Bulletin 122, 17–26. https://doi.org/10.1016/j.marpolbul.2017.05.012

Hydro, 2016. Hydrological Data Bank Hosted at the French Ministry of the Environment and of Sustainable Development. http://www.hydro.eaufrance.fr/index.php (Consulted in April 2016).

Kaberi, H., Tsangaris, C., Zeri, C., Mousdis, G.A., Papadopoulos, A., Streftaris, N., 2013. Microplastics along the shoreline of a greek island (kea isl., aegean sea)- types and densities in relation to beach orientation, characteristics and proximity to sources. Grafima Publ., Thessaloniki.

Käppler, A., Fischer, D., Oberbeckmann, S., Schernewski, G., Labrenz, M., Eichhorn, K.-J., Voit, B., 2016. Analysis of environmental microplastics by vibrational microspectroscopy: FTIR, raman or both? Analytical and Bioanalytical Chemistry 408, 8377–8391. https://doi.org/10.1007/s00216-016-9956-3

Kassambara, A., 2017. Ggpubr: 'Ggplot2' based publication ready plots. https://CRAN.R-project.org/package=ggpubr

Krelling, A.P., Williams, A.T., Turra, A., 2017. Differences in perception and reaction of tourist groups to beach marine debris that can influence a loss of tourism revenue in coastal areas. Marine Policy 85, 87–99. https://doi.org/10.1016/j.marpol.2017.08.021

Laglbauer, B.J., Franco-Santos, R.M., Andreu-Cazenave, M., Brunelli, L., Papadatou, M., Palatinus, A., Grego, M., Deprez, T., 2014. Macrodebris and microplastics from beaches in Slovenia. Marine Pollution Bulletin 89, 356–366. https://doi.org/10.1016/j.marpolbul.2014.09.036

Lavers, J.L., Bond, A.L., 2017. Exceptional and rapid accumulation of anthropogenic debris on one of the world's most remote and pristine islands. PNAS 201619818. https://doi.org/10.1073/pnas.1619818114

Lots, F.A., Behrens, P., Vijver, M.G., Horton, A.A., Bosker, T., 2017. A large-scale investigation of microplastic contamination: Abundance and characteristics of microplastics in European beach sediment. Marine Pollution Bulletin 123, 219–226. https://doi.org/10.1016/j.marpolbul.2017.08.057

Löder, M.G., Gerdts, G., 2015. Methodology used for the detection and identification of microplastics—A critical appraisal, in: Marine Anthropogenic Litter. Springer, pp. 201–227. https://doi.org/10.1007/978-3-319-16510-3_8

Ludwig, W., Serrat, P., Cesmat, L., Garcia-Esteves, J., 2004. Evaluating the impact of the recent temperature increase on the hydrology of the Têt River (Southern France). Journal of Hydrology 289, 204–221. https://doi.org/10.1016/j.jhydrol.2003.11.022

Ludwig, W., Dumont, E., Meybeck, M., Heussner, S., 2009. River discharges of water and nutrients to the Mediterranean and Black Sea: Major drivers for ecosystem changes during past and future decades? Progress in Oceanography 80, 199–217. https://doi.org/10.1016/j.pocean.2009.02.001

Maillet, G.M., Vella, C., Berné, S., Friend, P.L., Amos, C.L., Fleury, T.J., Normand, A., 2006. Morphological changes and sedimentary processes induced by the December 2003 flood event at the present mouth of the Grand Rhône River (southern France). Marine Geology 234, 159–177. https://doi.org/10.1016/j.margeo.2006.09.025

Mansui, J., Molcard, A., Ourmieres, Y., 2015. Modelling the transport and accumulation of floating marine debris in the mediterranean basin. Marine pollution bulletin 91, 249–257. https://doi.org/10.1016/j.marpolbul.2014.11.037

Mason, S.A., Garneau, D., Sutton, R., Chu, Y., Ehmann, K., Barnes, J., Fink, P., Papazissimos, D., Rogers, D.L., 2016. Microplastic pollution is widely detected in us municipal wastewater treatment plant effluent. Environmental Pollution 218, 1045–1054. https://doi.org/10.1016/j.envpol.2016.08.056

McDermid, K.J., McMullen, T.L., 2004. Quantitative analysis of small-plastic debris on beaches in the Hawaiian archipelago. Marine Pollution Bulletin 48, 790–794. https://doi.org/10.1016/j.marpolbul.2003.10.017

Moore, C.J., Moore, S.L., Leecaster, M.K., Weisberg, S.B., 2001. A Comparison of Plastic and Plankton in the North Pacific Central Gyre. Marine Pollution Bulletin 42, 1297–1300. https://doi.org/10.1016/S0025-326X(01)00114-X

Munari, C., Scoponi, M., Mistri, M., 2017. Plastic debris in the Mediterranean Sea: Types, occurrence and distribution along Adriatic shorelines. Waste Management 67, 385–391. https://doi.org/10.1016/j.wasman.2017.05.020

Murphy, F., Ewins, C., Carbonnier, F., Quinn, B., 2016. Wastewater Treatment Works (WwTW) as a Source of Microplastics in the Aquatic Environment. Environ. Sci. Technol. 50, 5800–5808. https://doi.org/10.1021/acs.est.5b05416

Napper, I.E., Thompson, R.C., 2016. Release of synthetic microplastic plastic fibres from domestic washing machines: Effects of fabric type and washing conditions. Marine Pollution Bulletin 112, 39–45. https://doi.org/10.1016/j.marpolbul.2016.09.025

OSPAR commission, 2010. Guideline for monitoring marine litter on the beaches in the ospar maritime area. OSPAR Commission (ISBN 90-3631-973).

Panno, S.V., Kelly, W.R., Scott, J., Zheng, W., McNeish, R. E., Holm, N., Hoellein, T.J., Baranski, E.L., 2019. Microplastic Contamination in Karst Groundwater Systems. Groundwater. https://doi.org/10.1111/gwat.12862

Pedrotti, M.L., Petit, S., Elineau, A., Bruzaud, S., Crebassa, J.-C., Dumontet, B., Martí, E., Gorsky, G., Cózar, A., 2016. Changes in the Floating Plastic Pollution of the Mediterranean Sea in Relation to the Distance to Land. PLOS ONE 11, e0161581. https://doi.org/10.1371/journal.pone.0161581

Poeta, G., Battisti, C., Bazzichetto, M., Acosta, A.T., 2016. The cotton buds beach: Marine litter assessment along the tyrrhenian coast of central italy following the marine strategy framework directive criteria. Marine pollution bulletin 113, 266–270. https://doi.org/10.1016/j.ecss.2016.08.041

Portman, M.E., Brennan, R.E., 2017. Marine litter from beach-based sources: Case study of an eastern mediterranean coastal town. Waste Management 69, 535–544. https://doi.org/10.1016/j.wasman.2017.07.040

Publithèque, 2016. Weather data bank hosted at Météo–France. https://publitheque.meteo.fr (Consulted in April 2016).

R Core Team, 2018. R: A language and environment for statistical computing. R Foundation for Statistical Computing, Vienna, Austria. https://www.R-project.org/

Reoyo-Prats, B., Aubert, D., Menniti, C., Ludwig, W., Sola, J., Pujo-Pay, M., Conan, P., Verneau, O., Palacios, C., 2017. Multicontamination phenomena occur more often than expected in Mediterranean coastal watercourses: Study case of the Têt River (France). Science of The Total Environment 579, 10–21. https://doi.org/10.1016/j.scitotenv.2016.11.019

Rochman, C.M., Tahir, A., Williams, S.L., Baxa, D.V., Lam, R., Miller, J.T., Teh, F.-C., Werorilangi, S., Teh, S.J., 2015. Anthropogenic debris in seafood: Plastic debris and fibers from textiles in fish and bivalves sold for human consumption. Scientific Reports 5, 14340. https://doi.org/10.1038/srep14340

Sadaoui, M., Ludwig, W., Bourrin, F., Raimbault, P., 2016. Controls, budgets and variability of riverine sediment fluxes to the gulf of lions (nw mediterranean sea). Journal of Hydrology 540, 1002–1015. https://doi.org/https://doi.org/10.1016/j.jhydrol.2016.07.012

Sanchez-Vidal, A., Canals, M., Calafat, A.M., Lastras, G., Pedrosa-Pàmies, R., Menéndez, M., Medina, R., Company, J.B., Hereu, B., Romero, J., Alcoverro, T., 2012. Impacts on the Deep-Sea Ecosystem by a Severe Coastal Storm. PLOS ONE 7, e30395. https://doi.org/10.1371/journal.pone.0030395

Serrat, P., Ludwig, W., Navarro, B., Blazi, J.-L., 2001. Spatial and temporal variability of sediment fluxes from a coastal Mediterranean river: the Têt (France). Comptes Rendus de l'Académie des Sciences - Series IIA - Earth and Planetary Science 333, 389–397. https://doi.org/10.1016/S1251-8050(01)01652-4

Schmidt, N., Thibault, D., Galgani, F., Paluselli, A., Sempéré, R., 2017. Occurrence of microplastics in surface waters of the Gulf of Lion (NW Mediterranean Sea). Progress in Oceanography. https://doi.org/10.1016/j.pocean.2017.11.010

Thompson, R.C., 2004. Lost at Sea: Where Is All the Plastic? Science 304, 838–838. https://doi.org/10.1126/science.1094559

Tubau, X., Canals, M., Lastras, G., Rayo, X., Rivera, J., Amblas, D., 2015. Marine litter on the floor of deep submarine canyons of the Northwestern Mediterranean Sea: The role of hydrodynamic processes. Progress in Oceanography 134, 379–403. https://doi.org/10.1016/j.pocean.2015.03.013

Turra, A., Manzano, A.B., Dias, R.J.S., Mahiques, M.M., Barbosa, L., Balthazar-Silva, D., Moreira, F.T., 2014. Three-dimensional distribution of plastic pellets in sandy beaches: Shifting paradigms. Scientific Reports 4. https://doi.org/10.1038/srep04435

Van Cauwenberghe, L., Devriese, L., Galgani, F., Robbens, J., Janssen, C.R., 2015. Microplastics in sediments: A review of techniques, occurrence and effects. Marine Environmental Research 111, 5–17. https://doi.org/10.1016/j.marenvres.2015.06.007

Wickham, H., 2017. Scales: Scale functions for visualization. https://CRAN.R-project.org/package=scales

Wickham, H., François, R., Henry, L., Müller, K., 2017. dplyr: A Grammar of Data Manipulation. https://CRAN.R-project.org/package=dplyr

Yang, D., Shi, H., Li, L., Li, J., Jabeen, K., Kolandhasamy, P., 2015. Microplastic pollution in table salts from China. Environ. Sci. Technol. https://doi.org/10.1021/acs.est.5b03163

Zubris, K.A.V., Richards, B.K., 2005. Synthetic fibers as an indicator of land application of sludge. Environmental Pollution 138, 201–211. https://doi.org/10.1016/j.envpol.2005.04.013

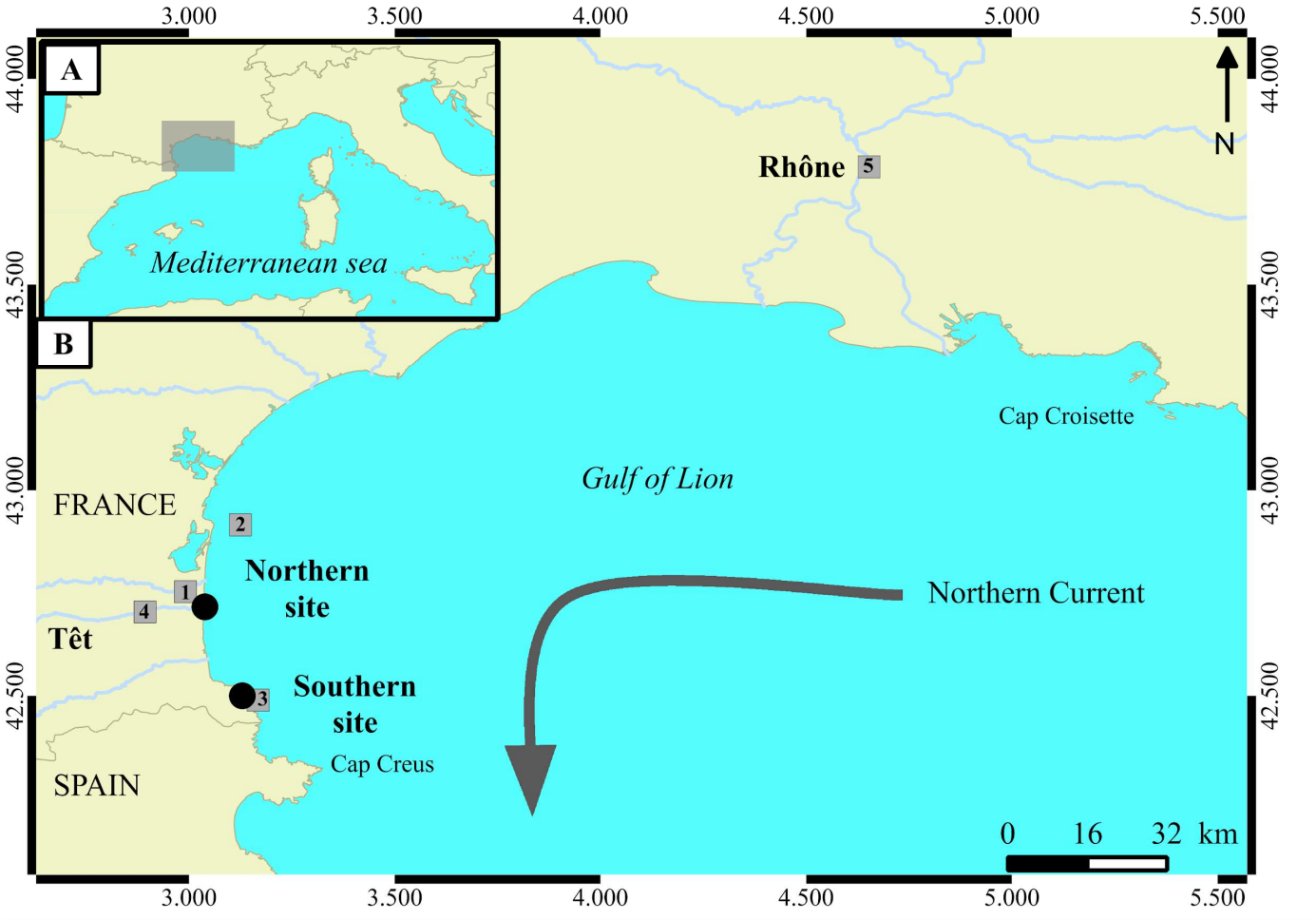

Figure 1. Location maps and main features of the study area. A) General map of the Northwestern Mediterranean Sea showing the location of the Gulf of Lion (shaded area). B) Location of the two investigated beaches in the southwestern Gulf of Lion (black dots). Grey numbered squares represent the weather station of Toreilles (1), the oceanographic buoys off Leucate (2) and Banyuls-sur-mer (3), and the gauging stations of Perpignan (4) and Arles (5) on the Têt and the Rhône rivers, respectively. The grey arrow indicates the mean flow of the Northern Current, representing the permanent mesoscale circulation of the Gulf of Lion.

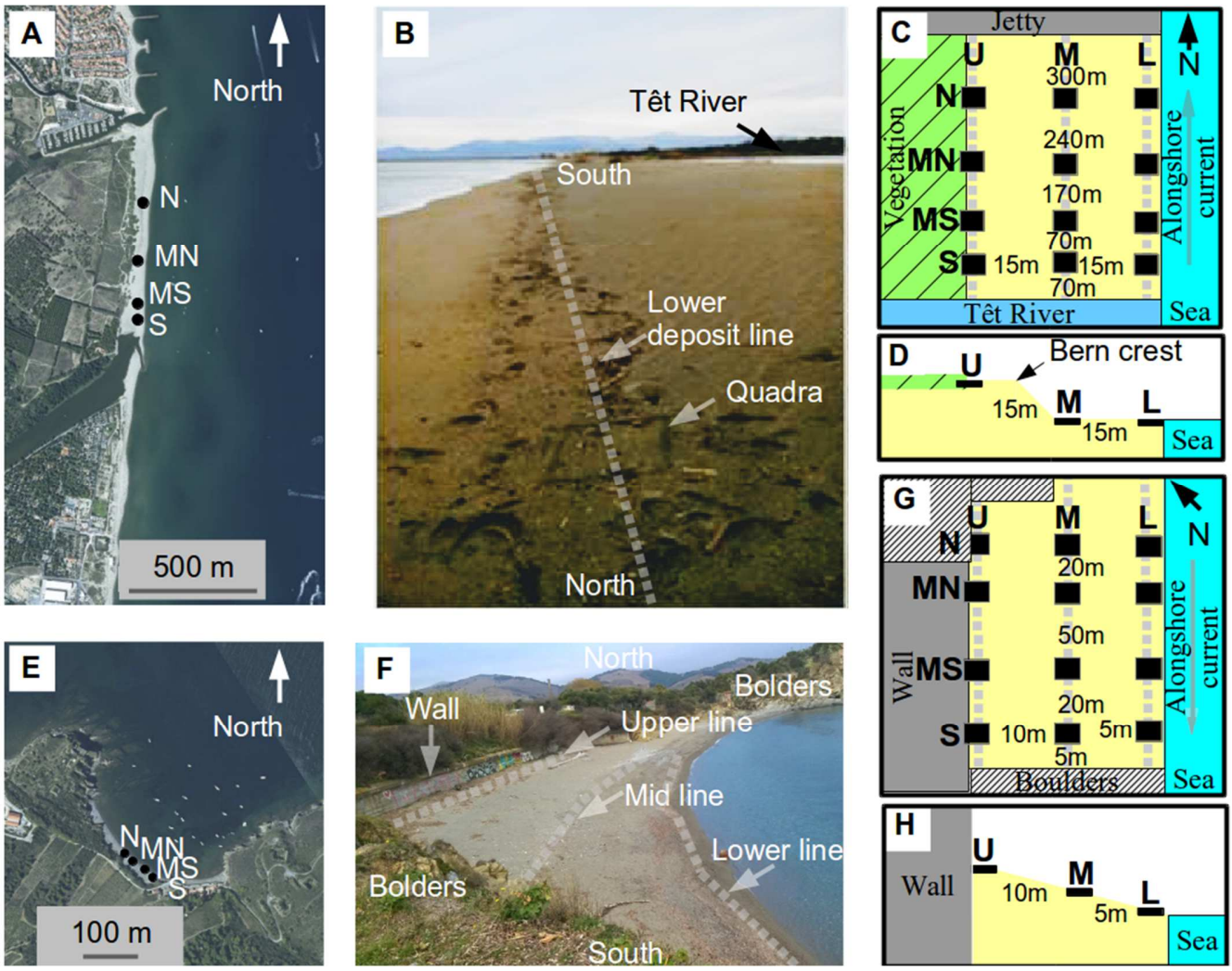

Figure 2. Aerial (A, E), on site pictures (B, F) and sketches (C, D, G, H) showing the sampling strategy for the northern (A to D) and the southern (E to H) sites. C and G are viewed from above, whereas D and H are cross-sections. Note the different scales of A, C and D (northern site) and E, G and H (southern site). Black squares represent the 12 sampling stations. Capital letters of A, C, E and G indicate the four cross-beach transects “North” (N), “Mid-North” (MN), “Mid-South” (MS) and “South” (S). Dotted lines of B, C, F and G represent the three alongshore beach transects performed along the deposit lines “Lower” (L), “Mid” (M) and “Upper” (U). Numbers of C and G indicate distance between quadrats in meters. Notice the opposite directions of the alongshore currents between the two sites (grey arrows).

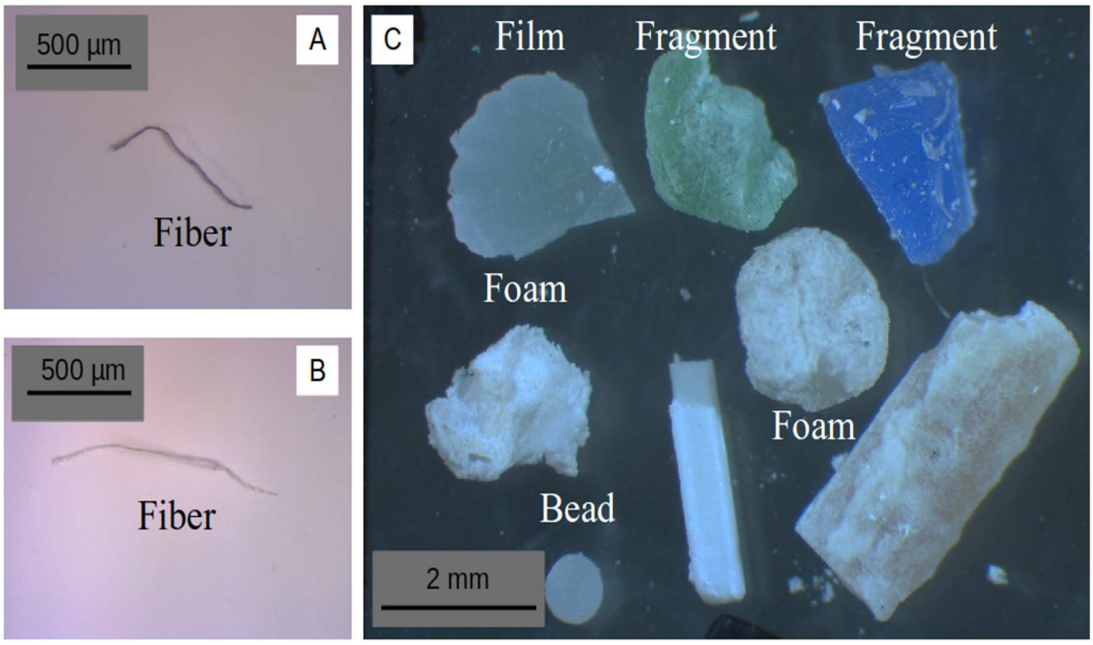

Figure 3. Examples of the five microplastic shape categories considered in the present study. A and B) Fibers. C) Film, fragments, foams and bead.

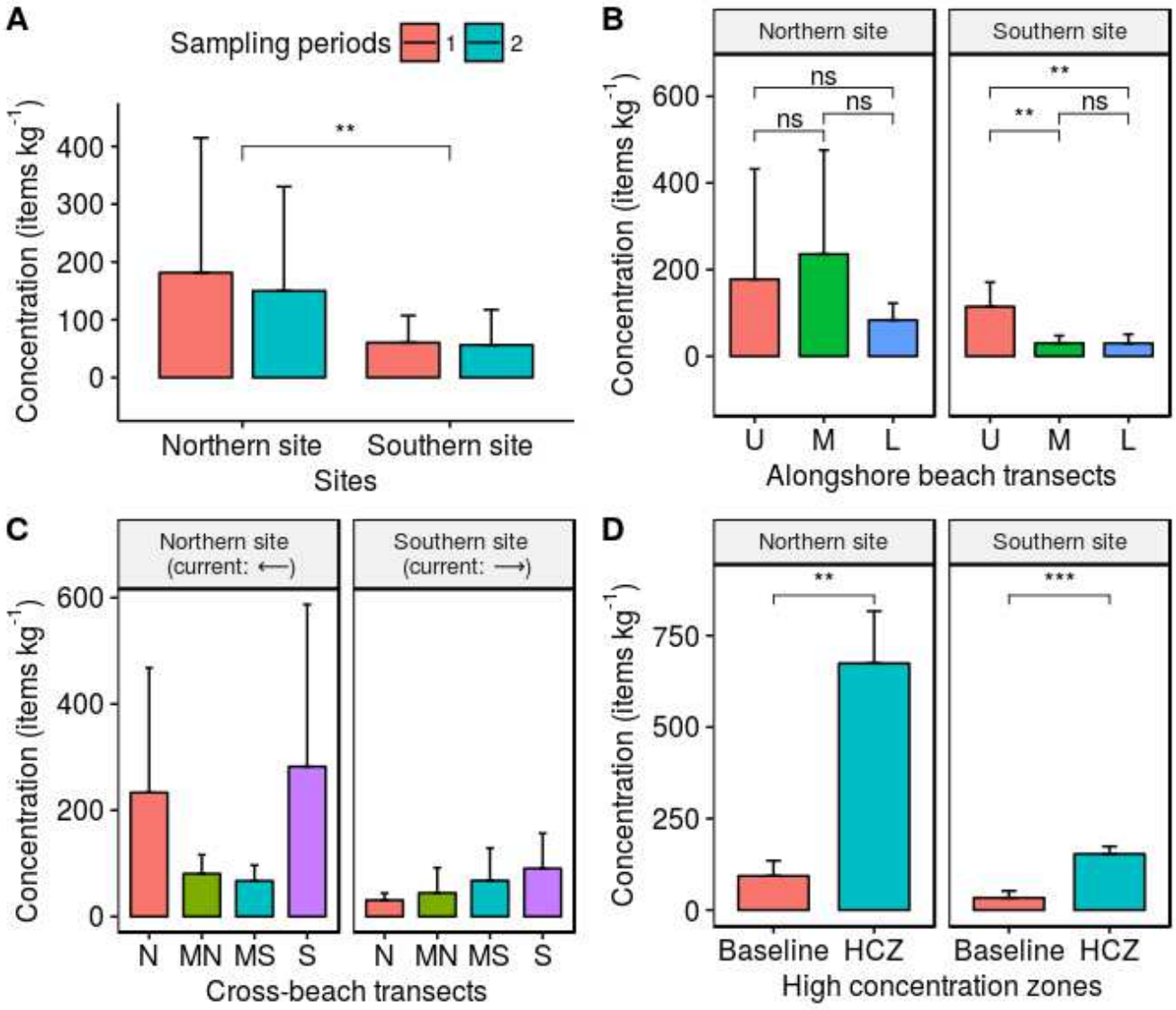

Figure 4. Mean MP concentrations ±1 SD per kg of dry sand (items kg^{-1}) and statistical significance of differences. A) Concentrations at the northern and the southern sites for the two sampling periods. B) Concentrations at the three alongshore transects for both study sites. C) Concentrations at the four cross-beach transects for both study sites. D) Comparison of concentrations between high concentration zones (HCZ) and the other sampling quadrats (Baseline) for both study sites. Alongshore transects: "Upper" (U), "Mid" (M) and "Lower" (L). Cross-beach transects: "North" (N), "Mid-North" (MN), "Mid-South" (MS) and "South" (S). See details in Figure 2). Bars represent the standard deviation from the means. ns: non significant difference (p-value >0.05). *: significant (p-value <0.05). **: Highly

significant (p-value <0.01). ***: very highly significant (p-value <0.001). See details about statistical tests in section 2.5.

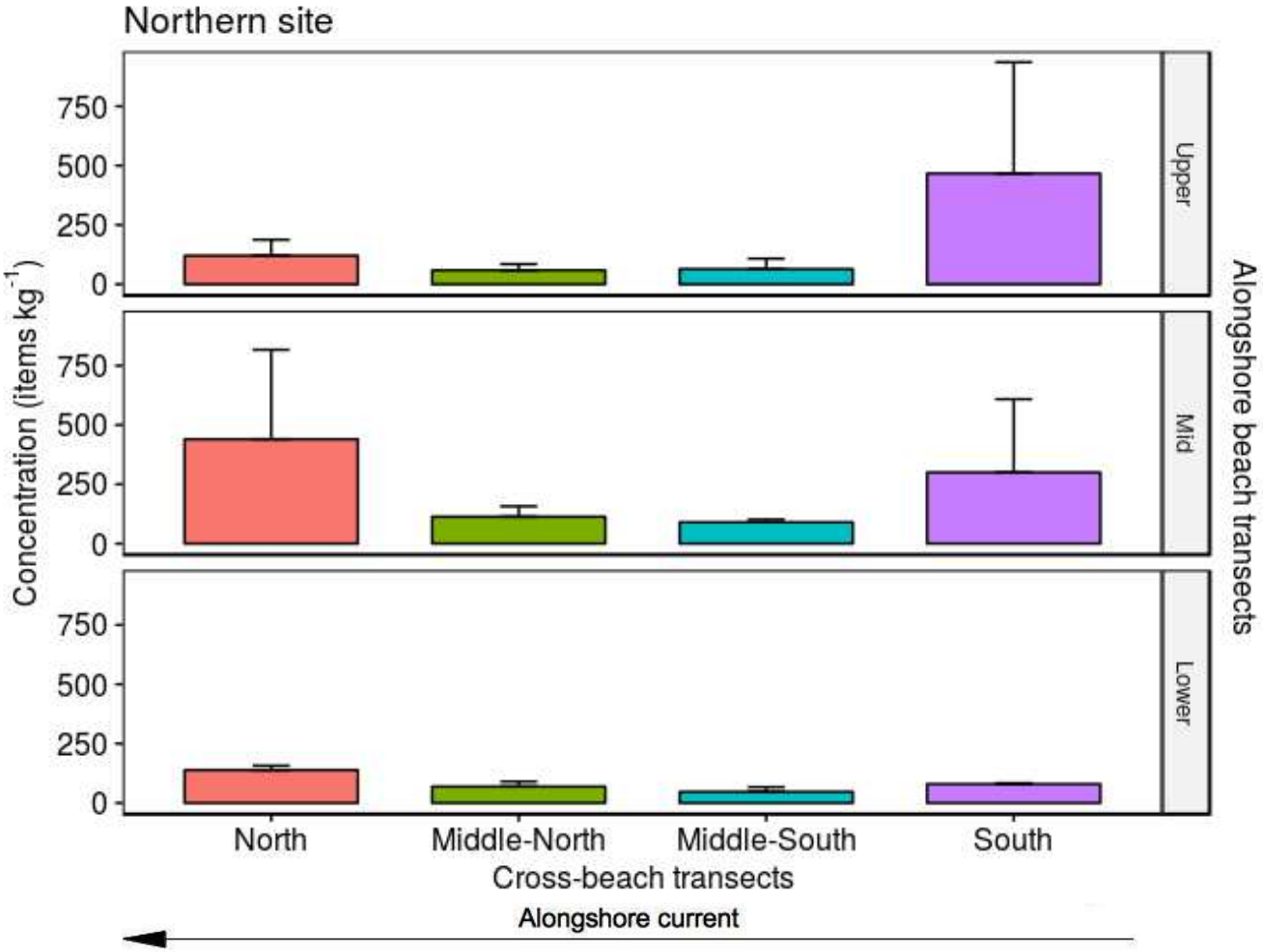

Figure 5. Mean MP concentrations ±1 SD (items kg^{-1}) at the northern site calculated for two sampling periods (March 2, 2016; March 30, 2016). Alongshore transects: “Upper” (U), “Mid” (M) and “Lower” (L). Cross-beach transects: “North” (N), “Mid-North” (MN), “Mid-South” (MS) and “South” (S). See details in Figure 2.

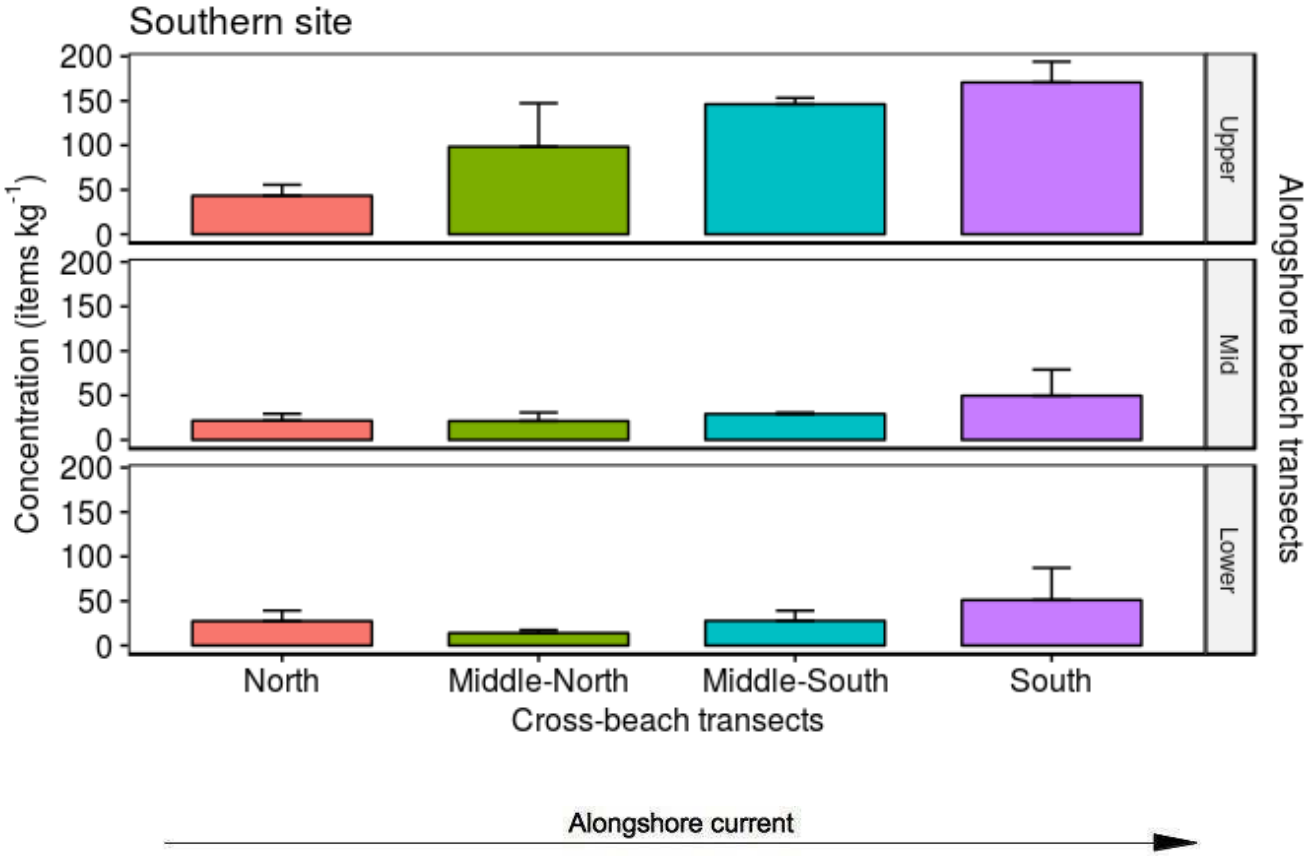

Figure 6. Mean MP concentrations ±1 SD (items kg^{-1}) at the southern site calculated for the two sampling periods (February 22, 2016; March 30, 2016). Alongshore transects: "Upper" (U), "Mid" (M) and "Lower" (L). Cross-beach transects: "North" (N), "Mid-North" (MN), "Mid-South" (MS) and "South" (S). See details in Figure 2.

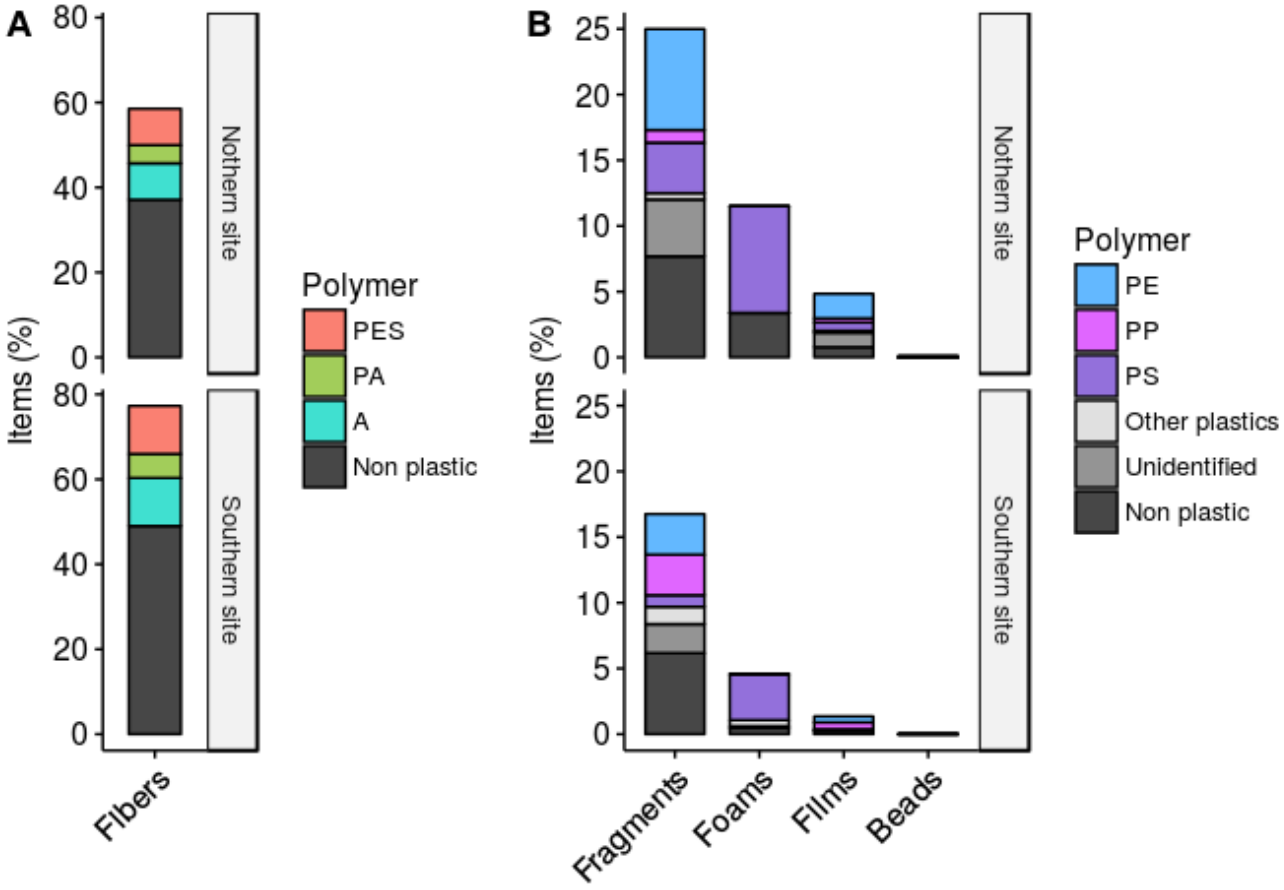

Figure 7. Shape distribution of MPs found on both sites (northern and southern data are pooled; Fig. 1) and synthetic organic polymer composition. A) fibers. B) fragments, foams, films and beads. Polymers: polyethylene (PE), polypropylene (PP), polystyrene (PS), polyester (PES), polyamide (PA), acrylic (A), other plastics (polyvinyl chloride, polyethylene-vinyl acetate, polyethylene terephthalate, polyurethane), unidentified and non plastics determined after FTIR spectroscopy analysis. See details in section 2.4. Notice the difference in % scale for fibers and for beads, films, foams and fragments.

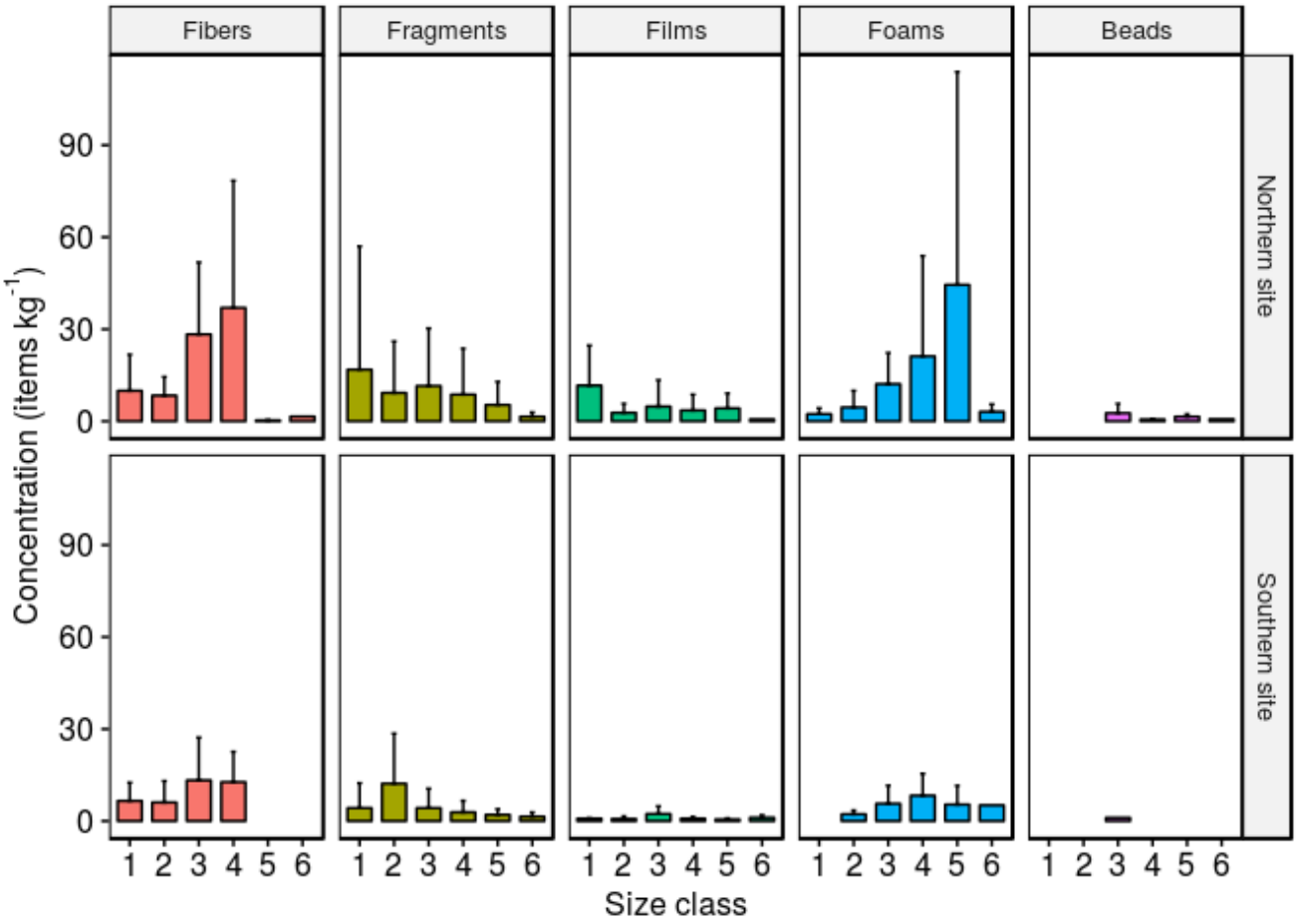

Figure 8. Mean MP concentrations ±1 SD (items kg^{-1}) of the different shape categories (fibers, fragments, films, foams, beads) within each sand size class (1: 0.063-0.315 mm ; 2: 0.315-0.5 mm; 3: 0.5-1 mm; 4: 1-2.5 mm; 5: 2.5-5 mm; 6: >5 mm).

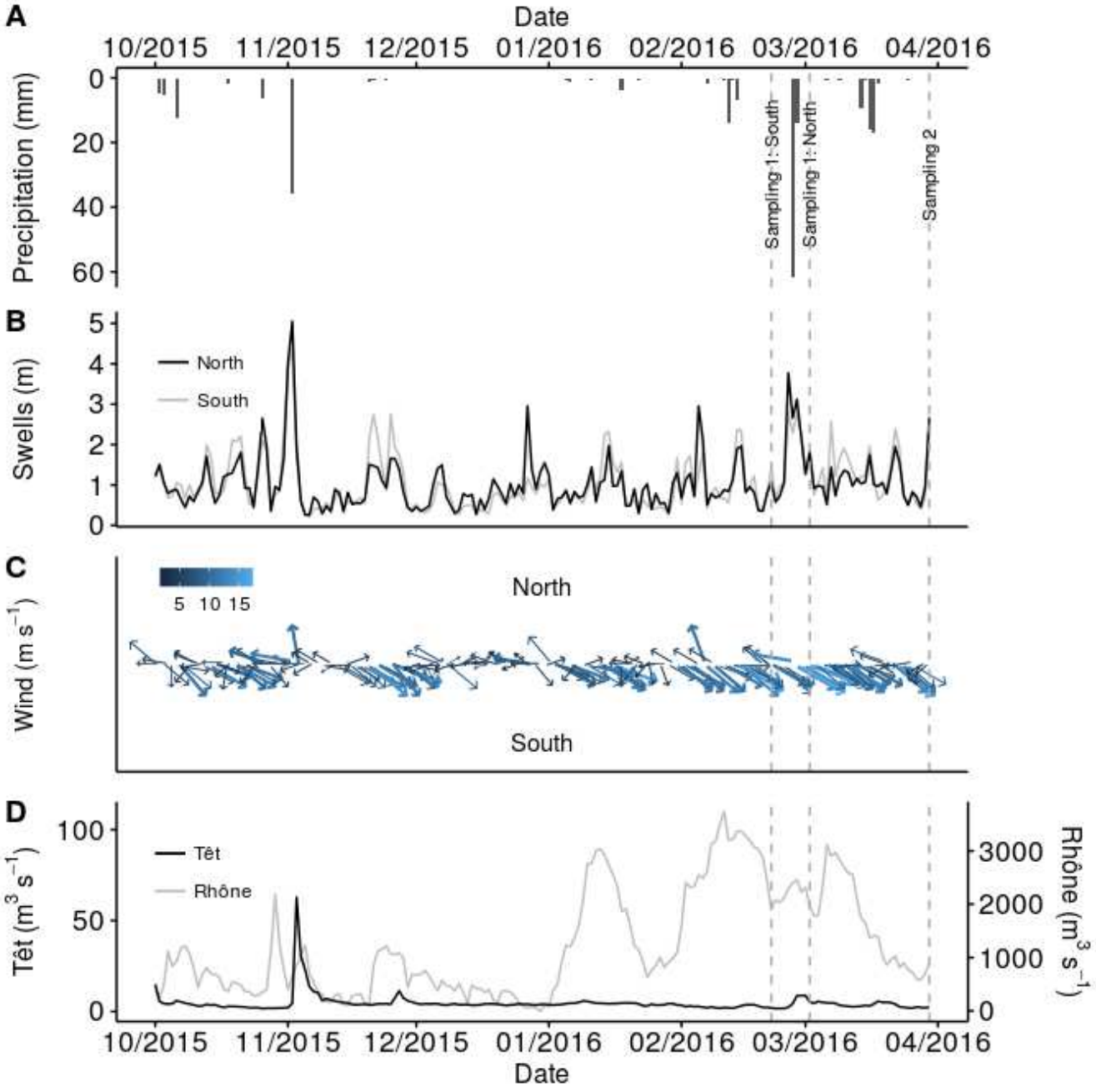

Figure 9. Meteorological and hydrological conditions prevailing before and during the sampling periods within the experimental area. A) Precipitation in mm, measured at Torreilles (42.3625 N, 2.6997 E; Fig. 1), data from Publithèque (2016). B) Maximum height of swell in m, northern site data measured at Leucate (2.9939 N, 42.7550 E), southern data at Banyuls-sur-mer (42.4895 N, 3.1677 E), data from CANDHIS (2016). C) wind speed (in m s^{-1}) and direction (North on the top) measured at Torreilles, data from Publithèque (2016). D) Têt and Rhône river outflow (m^3 s^{-1}; measured at Perpignan: 42.7034 N, 2.8930 E, and Beaucaire: 43.7877 N, 4.6529 E) data from Hydro (2016).

Table 1. Main features of the two sampled beaches in the southwestern part of the Gulf of Lion (NW Mediterranean Sea). Northern and southern sites are located 25 km apart (35 km alongshore).

	Northern site	**Southern site**
GPS coordinates	42.716758 N, 3.039624 E	42.499864 N, 3.128756 E
Beach size	700 m long x 70 m wide (49,000 m^2)	200 m long x 15 m wide (3,000 m^2)
Backshore boundary	Vegetation	Concrete wall and boulders
Touristic activity	High (mainly in summer)	High (mainly in summer)
River mouth	Têt	None
Shore type	Flat and sandy	Rocky with sand and gravel
Alongshore current direction	Northward	Southward

Table 2. Mean and range of MP concentrations (items kg^{-1} and items m^{-2} ±1 SD) collected within the two sites at both periods.

	Northern site		**Southern site**		
	Sampling 1	**Sampling 2**	**Sampling 1**	**Sampling 2**	**Unit**
Mean ± SD	182 ± 233	150 ± 180	60 ± 47	56 ± 61	Items kg^{-1}
	1,100 ± 1,629	*731 ± 528*	*254 ± 141*	*290 ± 292*	*Items m^{-2}*
Min	33	33	16	12	Items kg^{-1}
	145	*298*	*92*	*117*	*Items m-2*
Max	798	707	154	187	Items kg^{-1}
	4,653	*2,258*	*567*	*1,152*	*Items m^{-2}*
Total number of counted particles	6,366	5,370	1,928	2,000	Items
Identified plastic ratio	52	41	40	44	%
Total number of identified plastic items	3,301	2,192	763	871	items

Table 3. Factor analyses performed on all MP concentrations from both sites and sampling periods. *: significant (p-value <0.05). **: Highly significant (p-value <0.01). ***: very highly significant (p-value <0.001). See details about statistical tests in section 2.5.

Factors	**Northern site**	**Southern site**
Along-shore transects	0.16	<0.01 **
Cross-beach transects	0.06	0.15
Along-shore transects x Cross-beach transects	0.65	0.97

Table 4. Beached microplastics concentrations and polymeric composition observed along the Mediterranean coastline. Concentration values in brackets are maximum values. Decimal values are rounded to the nearest integer. ND: no data.

Country	Size range	Polymer analysis	% Fibers	Concentration	Reference
Items kg^{-1}					
Slovenia	0.25-5 mm	No	75%	178 (444)	Laglbauer *et al.,* (2014)
Italia	0.3-5 mm	70%PES, 20%PP, 10%PE (n=10)	99%	122	Lots *et al.,* (2017)
Spain				152	
France				124	
Italia				1,512	
Turkey				248	
Greece				232	
Israel				168	
Bosnia				76	
Italia	ND	38%PE, 35%PP, 12%Nylon, 9%PS, 4%PET, 2%PVC, <1%PUT (n=80)	10%	12 (22)	Munari *et al.,* (2017)
Tunisia	0.1-5 mm	Fragments : 86%PE, 14%PP; Fibers: 100%PP; Films & pellet: 100%PE; Foams: 100%PS (n=17)	71-99%	316	Abidli *et al.,* (2018)
France	0.063-5 mm	21%PS, 20%PES, 20%A, 12%PE, 10A%, 10%PP, <5% other plastics (n=114)	59%	166 (798)	This study: northern site
			77%	58 (187)	This study: southern site
Items m^{-2}					
Greece	1-2 mm	PE, PP, PET, PS	8%	ND (977)	Kaberi *et al.,* (2013)
	2-4 mm		0%	ND (1,218)	
France	0.063-5 mm	21%PS, 20%PES, 20%A, 12%PE, 10A%, 10%PP, <5% other plastics (n=114)	59%	915 (4,653)	This study: northern site
			77%	272 (1,152)	This study:

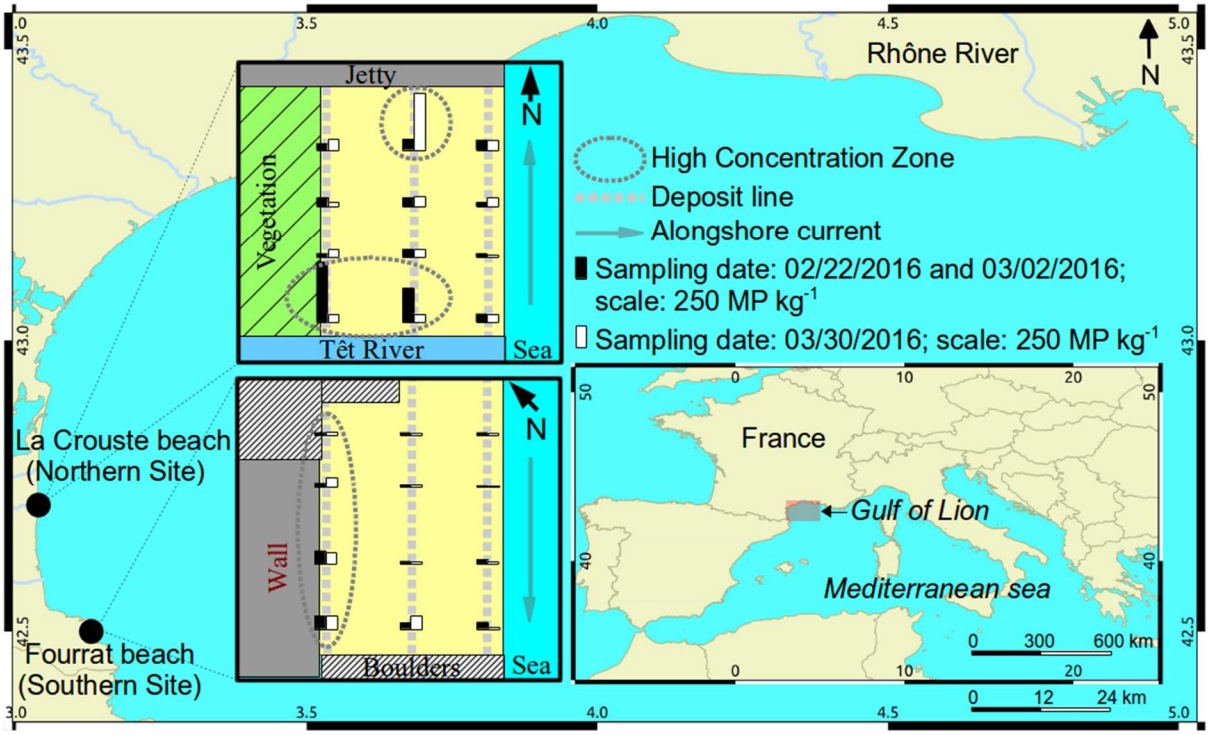
Rhône River
N
Jetty
Vegetation
Têt River
Sea
High Concentration Zone
Deposit line
Alongshore current
Sampling date: 02/22/2016 and 03/02/2016; scale: 250 MP kg-1
Sampling date: 03/30/2016; scale: 250 MP kg-1
La Crouste beach (Northern Site)
Fourrat beach (Southern Site)
Wall
Boulders
Sea
France
Gulf of Lion
Mediterranean sea
0 300 600 km
0 12 24 km